Auxetic Structure for Increased Power Output of Strain Vibration Energy Harvester

William J. G. Ferguson, Yang Kuang, Kenneth E. Evans, Christopher W. Smith and Meiling Zhu*

College of Engineering, Mathematics and Physical Sciences, University of Exeter, Exeter, UK, EX4 4QF
*Corresponding Author: M.Zhu@exeter.ac.uk

Abstract

This paper develops an auxetic (negative Poisson's ratio) piezoelectric energy harvester (APEH) to increase the power output when harnessing strain energy. The APEH consists of a piezoelectric element bonded to an auxetic substrate. The auxetic substrate concentrates the stress and strain into the piezoelectric element's region and introduces auxetic behaviour in the piezoelectric element, both of which increase the electric power output. A finite element model was developed to optimise the design and verify the mechanism of the power increase. Three APEHs were manufactured and characterised. Their performance was compared with two equivalent strain energy harvesters with plain substrates. Experimental results show that the APEHs, excited by sinusoidal strains peak-to-peak of 250 με at 10 Hz, are able to produce electric power of up to 191.1 μW, which is 14.4 times of the peak power produced by the plain harvesters (13.4 μW). The power gain factor is constant between samples as the amplitude and frequency of their applied strains are varied. The model and experimental results are in good agreement, once accounting for the imperfect bonding of the epoxy using the spring constant of the Thin Elastic Layers on the modelled epoxy surfaces.

Keywords: Vibration Energy Harvesting; Auxetic; Piezoelectricity; Strain Energy Harvesting

1. Introduction

Energy harvesting is concerned with utilising small amounts of energy available within the local environment to power small electronic devices [1–3]. Popular potential applications of this technology include self-powered sensor nodes in a distributed wireless network, typically used for structural health monitoring. Being powered in-situ means these sensors won't require routine battery replacement, and can thus be embedded into a structure or benefit from quick, easy, and flexible retrofitting without additional (re)wiring [4,5]. Given adequate power availability, this technology could recharge mobile devices on the move. Other applications such as powering wireless switches, doorbells and security equipment [6], keyboards [7], and asset management trackers [8,9] are being explored.

In some cases, ambient vibration energy in buildings, vehicles or machinery may be sufficient to provide power to such a device via a harvesting mechanism such as piezoelectricity [10,11]. Many vibration energy harvesters use the inertia of a proof mass to help couple the energy into the electro-mechanical transduction mechanism, which could be piezoelectric, electromagnetic, triboelectric, or electrostatic [1–3]. Most inertial harvesters are dependent on a resonant frequency for optimum power output, outside which there will be a significantly reduced output. Alternatively, strain energy harvesting avoids any reliance on the harvester's resonant condition, and can be achieved by a piezoelectric material bonded to the vibrating structure; its simple implantation, ease of scaling up, and no moving parts make strain energy harvesting an attractive option for vibration energy harvesting [11,12].

Strain energy harvesting is attractive where the 'skin' of a structure is under variable loading, such as the wing of a plane [4,11,12]. For safety reasons, the amplitude of the dynamic strains are designed to keep to a minimum (for example, 300 με (micro-strain) would generally be considered high [12]). This low strain amplitude limits the power output of the strain energy harvester. One way to harvest more strain energy while minimising impact on the host structure would be to use auxetic materials in the harvester.

Auxetic materials and structures possess a negative Poisson's ratio, meaning they expand laterally under tension (or contract laterally under compression), in direct contrast to conventional materials [13–21]. Most innately auxetic materials have infolding internal structures, meaning they would lack the authority to stretch a stiffer material bonded to them (such as most piezoelectric materials). There are however various structures that can give a stronger bulk material auxetic behaviour, resulting in a negative effective Poisson's ratio while possessing more authority. One of the more widely discussed structures, the re-entrant honeycomb array (REHA), is shown in Figure 1 [13–17,20]. It is based on a hollow hexagonal network with two opposing corners pushed inwards until they re-enter the hexagon; this leaves an hourglass-shaped hole in the centre. When this structure is placed under tension these holes open up (tending toward rectangles) and the beams push outward [17].

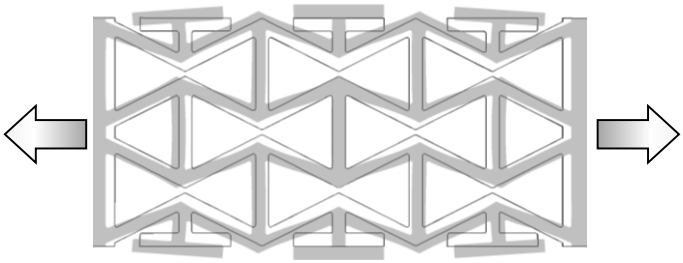

Figure 1: Example auxetic structure: re-entrant honeycomb array (REHA). Arrows show the axial stretch direction, deformed result shown in grey (magnified for clarity) compared to its original shape shown in the black outline.

The use of auxetic elements in energy harvesting is still at an early research stage. Li, Kuang and Zhu [22] have modelled a bimorph energy harvester with an auxetic substrate. This could generate 2.76 times the power of an equivalent plain form, i.e. a solid substrate with the same external dimensions, by engaging both the conventional 31-mode and the generally neglected 32-mode of the piezoelectric elements.

De Bellis and Bacigalupo [23] have modelled and analysed an anti-tetrachiral auxetic lattice which could form the active part of a self-powering and more sensitive strain gauge. Their piezoelectric element (PZT-5A) is sandwiched by polymeric material, with the same auxetic profile through the thickness; this makes the device more flexible than bulk PZT, increasing its response to an applied strain.

Umino, et al. [24] have modelled and demonstrated a MEMS bimorph energy harvester using a REHA auxetic substrate which generated 1.6 times more power than one with a plain plate. Their auxetic substrate reduces their bimorph's rigidity which allows for a greater flexing and thus a greater power output from the attached piezo-elements (PVDF). This substrate also reduces its resonant frequency compared to the plain; by adjusting the substrate structure, the resonant frequency may be tuned independently from the bimorph's overall size, as shown by Adeshara [25], Chandrasekharan and Thompson [26].

There has been some related work in piezoelectric auxetic actuators, some of which could be run in reverse as energy harvesters. Fey, et al. [27], have demonstrated an auxetic REHA actuator made of PZT to increase the displacement from an applied voltage; this could potentially be run in reverse as an energy harvester. Being made of only bulk ceramic, this would be liable to cracking under excessive loads if used in this manner.

In this study, we developed a piezoelectric strain energy harvester incorporating auxetic structure to increase the electrical power output. This auxetic piezoelectric energy harvester (APEH) uses a substrate with an auxetic region to introduce auxetic behaviour and concentrate stress in the piezoelectric element. The APEH could be used in the future to power wireless sensor nodes for structural health monitoring in buildings and vehicles.

2. Auxetic Energy Harvester

The auxetic piezoelectric energy harvester (APEH) proposed in this study is schematically shown in Figure 2. It consists of one or two d_{31}-mode piezoelectric elements bonded to either face of a substrate, which is then fixed onto a host structure. The region of the substrate sandwiched between the piezoelectric elements has been formed into an auxetic structure. The advantage of this auxetic region is twofold: firstly, the auxetic region can stretch the piezoelectric element in two directions at once and thus increase the electric power output; secondly, the auxetic region has a lower stiffness than the rest of the substrate, which concentrates the stress into the piezoelectric elements. This concentration effect helps to increase the power density of the energy harvester.

Figure 2: Schematic of the auxetic piezoelectric energy harvester (APEH) bonded over a host structure, the source of vibrations. A second piezo element could be added on the underside of the auxetic region.

When a uniaxial strain is applied to the substrate at frequencies far below its resonance frequency, the piezoelectric power output can be formulated as [22]:

$$P_{opt} = \frac{f\, A_p\, t_p\, d_{31}^2}{\varepsilon_0 \varepsilon_{33}} \left(\overline{\sigma_{11}} + \overline{\sigma_{22}}\right)^2 \quad (1)$$

where f is the excitation frequency; A_p and t_p are the area and thickness of the piezoelectric material; d_{31} is the piezoelectric charge constant, note that for bulk ceramic: $d_{31} = d_{32}$; ε_{33} is the piezo's relative permittivity; $\overline{\sigma_{11}}$ and $\overline{\sigma_{22}}$ are the average axial (*x*-axis) and lateral (*y*-axis) stresses in the piezoelectric material respectively.

Eq. (1) suggests that $\overline{\sigma_{11}}$ and $\overline{\sigma_{22}}$ contribute equally to power generation. For conventional strain harvesters, the Poisson's ratios of the piezoelectric material and the substrate are both positive, and of similar value; they therefore contract transversely at about the same rate when stretched. There is thus little external lateral force applied on the piezo and $\overline{\sigma_{22}}$ arises primarily from the piezo's own Poissonian contraction. This makes it the opposite sign to, and smaller than, $\overline{\sigma_{11}}$ and it is only considered for its retardant effect. The $\overline{\sigma_{11}}$ term therefore dominates the power output for a conventional strain harvester. If the substrate has a negative Poisson's ratio however, and thus expands laterally under tension, it will apply this lateral force on the piezo element. As a result, $\overline{\sigma_{22}}$ will increase (and, if the force is sufficient, will take on the same sign as $\overline{\sigma_{11}}$), therefore both $\overline{\sigma_{11}}$ and $\overline{\sigma_{22}}$ can contribute to the power generation simultaneously.

To introduce auxetic behaviour in the substrate, our APEH substrate incorporates a re-entrant honeycomb structure, similar to that shown in Figure 1. For the present study, a single re-entrant hexagonal unit was used for a small scale harvester.

3. Finite Element Modelling

3.1. FE Modelling Method

Finite element (FE) modelling was used to investigate the benefits of the auxetic region on the harvested power. The FE model, developed in COMSOL Multiphysics® 5.3, is schematically illustrated with an exploded view in Figure 3(a) and isolated auxetic region in Figure 3(b). The model consists of a steel substrate, with a re-entrant honeycomb unit as auxetic region, and a piezoelectric element (PIC151, Physik Instrumente). An epoxy layer of 8 μm thick is included between these components. The dimensions and material properties of the model are listed in Table 1 and Table 2, respectively.

The substrate has two clamped portions, each with a length of L_{clp}, at either end. In the model, one clamped portion was fixed, while the other was subjected to an axial harmonic displacement to produce an overall strain of 250 με at 10 Hz on the free portion of substrate. A load resistor was connected across the electrodes on the top and bottom faces of the piezoelectric element. Its resistance was set using Eq. (2) to match the internal impedance of the PZT, to characterise the maximum available electric power output.

$$R = \frac{t_p}{2\pi f \varepsilon_0 \varepsilon_{33} A_p} \tag{2}$$

To demonstrate the benefits of the auxetic region for energy harvesting, an equivalent plain energy harvester was also modelled. It uses a plain bulk substrate with the same external dimensions as the auxetic model, but has no auxetic region. The piezoelectric element remains the same, and the epoxy layer fills the whole area under it.

A parametric analysis was performed to determine the optimal dimensions of the auxetic region, which gave the maximum power output while keeping the peak stress within the material strength (with a safety factor of 1.3). The parameters studied include: beam width t_b, cell angle α, crossbeam length cb, and filleting radius r, all shown in Figure 3(b)). The studied ranges and the optimised values of these parameters are listed in Table 1. Detailed results of the parametric studies may be found in the Supplementary Material.

To account for imperfections in the adhesive's bonding, thin elastic layers (TELs) were included at the epoxy's interfaces with both the substrate and the piezoelectric element. The TELs are a spring boundary condition available in COMSOL which connects the touching faces purely via visco-elastic forces, proportional to their relative displacement and velocity. The stiffness per unit area in the TELs, k_a, represents the bonding strength of the layer; a higher spring constant corresponding to a stronger bond. The value of k_a was indeterminable prior to the experiment, but for the purposes of the design stage it was estimated to be in the order of 100 GN/m^3. This value was derived by comparing the power outputs of Pozzi et al. [11] (using similar piezoelectric elements to ours) with the plain version of the model using a range of k_a values (shown in Figure 5(a)). An improved value of k_a for future modelling and design work may be determined from experiment, as in Section 5.2.1.

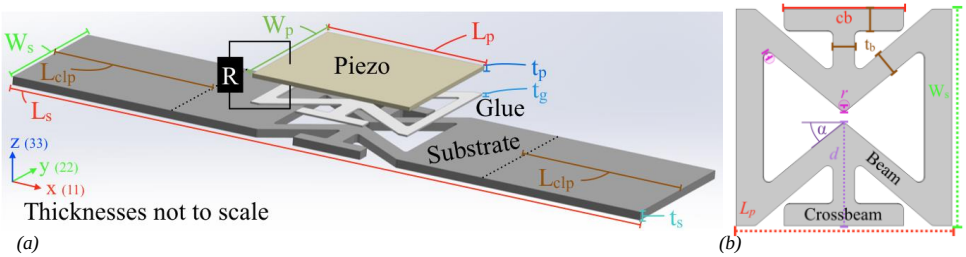

Figure 3: (a) Exploded render of model, annotated with external parameters and (b) parameters for the auxetic region (i.e. area of substrate directly under the piezo). Parameter values are listed in Table 1.

Table 1: Parameter values used in the model (final value given with modelled ranges where applicable)

Part	Parameter	Symbol	Value (range)	Unit
Piezo-Element	Length	L_p	20	mm
	Width	W_p	20	mm
	Thickness	t_p	180	μm
	Resistance	R	465	kΩ
Epoxy	Thickness	t_g	8	μm
	TEL	k_a	100	GN/m^3
Substrate	Length	L_s	80	mm
	Width	W_s	20	mm
	Thickness	t_s	1.15	mm
	Clamp	L_{clp}	20	mm
Auxetic Region	Beam Width	t_b	2 (1–3)	mm
	Cell Angle	α	33 (1–42)	°
	Deformation*	d	7.4 (1–9.8)	mm
	Crossbeam	cb	11 (2–12.1)	mm
	Fillet Radius	r	0.5 (0.1–1.3)	mm

** Deformation length, d, derived from α and t_b*

Table 2: Material properties used in the model.

Material	Property		Value	Unit
PZT: PIC151 (Piezo-Element) [28]	Density	ρ_p	7500	kg/m^3
	Compliance Matrix	s_{11}^E	16.83	μm^2/N
		s_{33}^E	19.00	μm^2/N
		s_{55}^E	50.96	μm^2/N
		s_{12}^E	-5.656	μm^2/N
		s_{13}^E	-7.107	μm^2/N
		s_{44}^E	50.96	μm^2/N
		s_{66}^E	44.97	μm^2/N
	Coupling Matrix	d_{31}	-214.0	pC/N
		d_{33}	423.0	pC/N
		d_{15}	610.0	pC/N
	Relative Permittivity	ε_{11}	1936	–
		ε_{33}	2109	–
Epoxy	Density	ρ_g	1250	kg/m^3
	Poisson's Ratio	ν_g	0.35	–
	Young's Modulus	E_g	1.00	GPa
Steel: EN 10130 (Substrate)	Density	ρ_s	7870	kg/m^3
	Poisson's Ratio	ν_s	0.29	–
	Young's Modulus	E_s	200	GPa

3.2. FE Modelling Results

The APEH with the optimised dimensions produced electric power of 66.8 μW when excited by strains of 250 με at 10 Hz, with a k_a of 100 GN/m^3. Compared to the power of 5.8 μW produced by the equivalent plain harvester, the APEH shows a power gain of 11.5 times. The power gain remained constant when the amplitude and frequency of the excitation strain are varied. To verify the mechanism of the power increase, the stress in both harvesters was examined, as shown in Figure 4.

The plain substrate has its stress distributed evenly in the areas between the two clamping portions (Figure 4(a)). In contrast, the auxetic substrate concentrates the stress and strain into the more pliable auxetic region, particularly into those corners which flex outward. The peak stress of 216 MPa in the APEH was therefore found at the apex of one of these corners. This stress is sufficiently below the yield strength (280 MPa) of the substrate. The peak stress in the piezoelectric element was found to be around 10 MPa, less than a third of its tensile strength (35 MPa).

As a result of the stress concentration in the APEH, its piezoelectric element experiences an average axial stress, $\overline{\sigma_{11}}$, of 3.0 MPa. This is notably higher than the 1.9 MPa for the equivalent plain harvester. Meanwhile the average lateral stress in the APEH's piezoelectric element, $\overline{\sigma_{22}}$, is 1.8 MPa. This, like its axial stress, is tensile, which demonstrates the auxetic behaviour of the APEH. In contrast, the average lateral stress of the piezoelectric element in the plain harvester is -0.46 MPa; the negative here indicates typical Poissonian contraction.

Considering Eq. (1), the increased axial stress combined with the change in the sign of lateral stress leads to the power increase of the APEH. The values of $(\overline{\sigma_{11}} + \overline{\sigma_{22}})^2$ from Eq. (1) for the APEH and plain harvesters are 23.8 and 2.07 MPa^2, respectively. These give a power gain of 11.5; this agrees with the FEM simulated power gain. Therefore, the power increase in the APEH is caused by the combined effects of stress concentration and auxetic behaviour of the auxetic region.

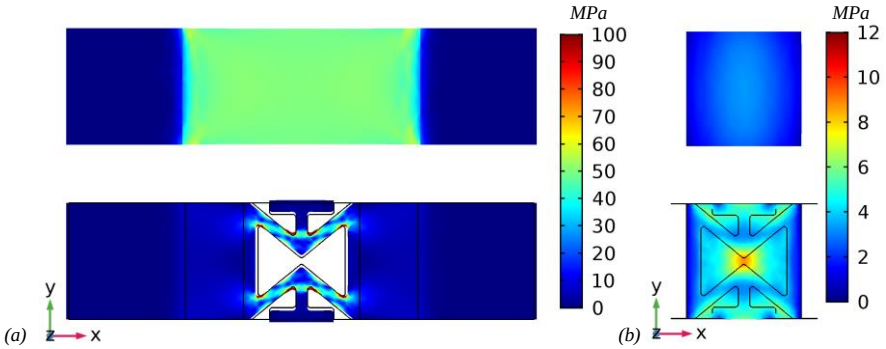

Figure 4: False colour image of (a) substrate and (b) PZT stress distributions in the Plain (top) and Auxetic (bottom) models. Colour ranges capped and deformations (compared to outlines) shown magnified 100 times for clarity.

Since the epoxy's bonding strength could only be estimated prior to the experiment, its potential effect on the performance of the energy harvesters was studied using the value of spring constant per unit area, k_a, in the TELs. This is presented in Figure 5. As k_a increases, the epoxy layer transfers the strain on the substrate into the piezoelectric element more efficiently. As a result, an increase in the stress and power output is observed in both auxetic and plain harvesters. Using Figure 5(a) we are able to use a sample's measured power output to estimate the associated k_a value; this can then be used as a starting point in future models. If the k_a value is significantly higher than our estimate then the same excitation could cause excessive stress in the piezoelectric element, as indicated by Figure 5(b), highlighting the effect of bonding strength on the energy harvesters.

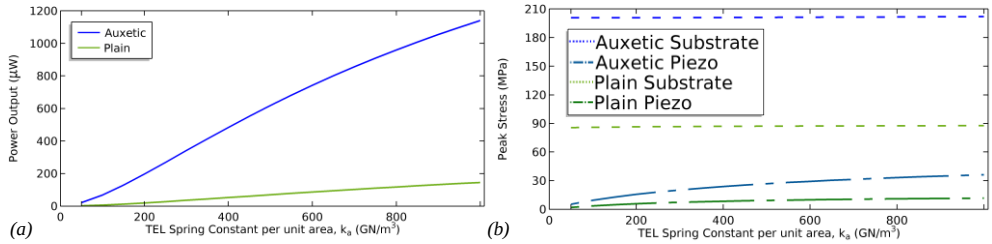

Figure 5: Simulated (a) power output and (b) peak stresses of Auxetic and Plain harvester designs against spring constant per unit area, k_a, in their Thin Elastic Layers. All points use the same excitation of 250 $\mu\varepsilon$ at 10 Hz.

4. Manufacture of Harvester Samples

The manufacture of the harvester samples started by laser-cutting a mild steel sheet (BS EN 10130) to the shape of the substrates, either plain or auxetic, as designed in Section 3 and defined by the dimensions in Table 1. Epoxy resin (Scotch-Weld™ 460) was applied to the substrate surface and then the piezoelectric element (PIC151, Physik Instrumente) was placed over it. Excess epoxy was removed where accessible. The samples were then clamped firmly in a vice for over 24 hours while the epoxy cured at room temperature. Finally, wires were soldered to the electrode surfaces of the PZT. In total, three auxetic and two plain samples were made and characterised.

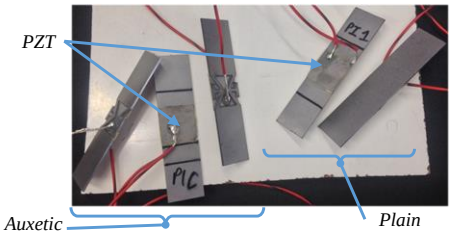

Figure 6: Three Auxetic (right) and two Plain (left) samples after epoxy is cured and wires attached.

5. Experimental Characterisation

5.1. Experimental Method

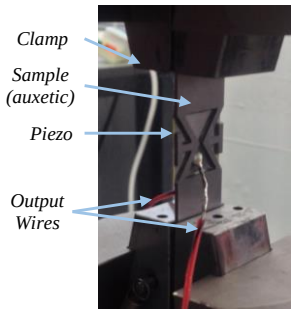

Figure 7: Auxetic piezoelectric energy harvester installed on the material testing machine for characterisation.

For the experimental characterisation, the harvester samples were clamped by a material testing machine (Instron ElectroPlusTM E10000) to depth of approximately 20 mm on each end, as shown in Figure 7. The material testing machine applied a harmonic strain to the sample at an amplitude of 250 με peak-to-peak (i.e. a peak extension of 10 μm) at a frequency of 10 Hz. The applied harmonic strain was set up so that the energy harvester would remain in tension throughout the excitation to avoid buckling. The output wires of the energy harvester were connected to a variable resistor (1-999 kΩ). The voltage across this variable resistor was recorded by a data log (National Instrument cDAQ-9174 with NI 9229 card). The total load resistance, R, is then the variable resistor in parallel with the 1 MΩ input impedance of the data log. To find the average generated power, the instantaneous power was calculated ($P_i = V_i^2/R$), and integrated with respect to the time to find the accumulated energy. The gradient of the accumulated energy is approximately linear once the Instron achieves a steady state excitation; this gradient is the average power output of the trial.

5.2. Results and Discussion

5.2.1. Increased Power Output

Figure 8 shows the experimental results from the two plain and three auxetic harvester samples, excited at 250 με and 10 Hz, alongside their corresponding simulation results. Table 3 summarises the measured optimum characteristics of the energy harvesters: load resistor R and power P_{opt}, the power gain, and associated k_a.

The auxetic samples produced peak power of 121.9 to 142.2 µW, compared to 13.4 and 13.2 µW by the plain harvesters. The power gain is between 9.2 and 14.4, with a mean value of 11.4 among the three auxetic samples. Wide variations in the measured power output are observed between the auxetic samples, while the plain ones show a much more consistent power output. This variation is caused primarily by excess epoxy leaking into the corners of the auxetic region during curing, increasing the stiffness of the auxetic region to an uncontrollable degree. This variation can be emulated in the simulation by using k_a. With the data presented in Figure 5(a), a sample's optimum power output may be paired with an associated k_a value. The simulated power then approximately matches the experiments', as shown in Figure 8.

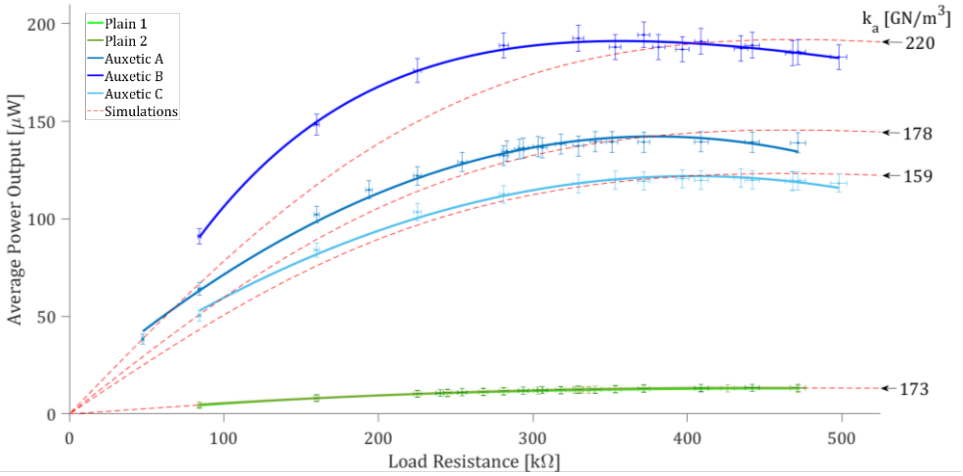

Figure 8: The experimental and simulated power output from all five harvester samples against electrical load resistance, when excited at 250 µε, 10 Hz. Corresponding FE simulation for each sample shown with its TEL's k_a value.

Table 3: Measured characteristics of the plain and auxetic harvester samples.

Sample	R (kΩ)	P_{opt} (µW)	Gain	k_a (GN/m^3)
Plain 1	463	13.4	—	173
Plain 2	472	13.2	—	173
Auxetic A	382	142.2	10.7	178
Auxetic B	360	191.1	14.4	220
Auxetic C	402	121.9	9.2	159

5.2.2. Effects of Input Excitations

The effects of the strain amplitude and frequency on the performance of the energy harvesters are presented in Figure 9. The experiment results were obtained from auxetic sample B and plain sample 1. The values of k_a for auxetic and plain harvesters in their simulations were maintained at 220 and 173 GN/m^3, respectively. When the frequency was varied for Figure 9(a), the strain amplitude was kept constant at 250 µε peak-to-peak. When the peak-to-peak strain amplitude was varied for Figure 9(b), the applied frequency was kept constant at 10 Hz.

As may be observed from Figure 9, in both simulation and experiment, the power outputs of the harvesters increase approximately linearly with frequency and quadratically with the strain amplitude, as expected from Eq. (1). The simulated power is in good agreement with experiment, suggesting k_a approximates the imperfect bonding across this range of excitations. In both cases the power gain is approximately constant at about 14.5 across the excitation range. This indicates that the gain factor is a product of the substrate geometry rather than of the excitation. Other samples exhibited the same behaviour, but are omitted for clarity.

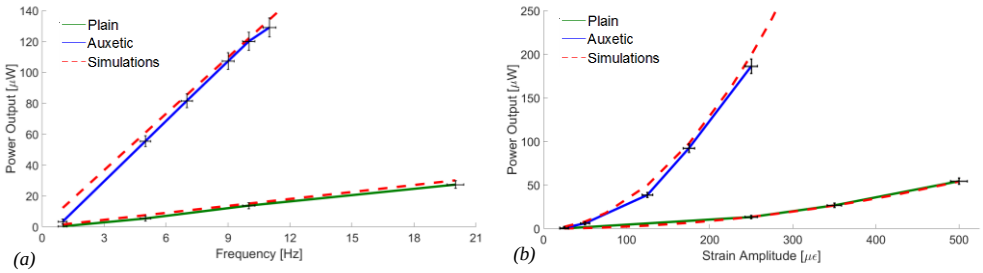

Figure 9: Measured and simulated results of (a) strain frequency and (b) strain amplitude on harvester's power output.

When a strain of 275 με was applied to the auxetic samples, a hairline crack formed across the PZT. The original design simulations, discussed in Section 3 and the Supplementary Material, predicted the piezoelectric element should be able to sustain an excitation strain of ~400 με on the auxetic sample before reaching its tensile strength of 35 MPa, but this prediction used the estimated k_a of 100 GN/m^3. Using the experimentally established value of 220 GN/m^3 (for sample B), a revised simulation predicts that the stress in the piezoelectric element should be tolerable up to a ~330 με excitation, which is still higher than the experimental outcome here. This discrepancy is likely due to minor defects in the PZT or imperfections introduced during manufacture. This indicates a greater margin for error should be introduced when considering the integrity of the auxetic harvesters.

The latter result indicates that use of auxetic elements in strain energy harvesting should be restricted to well characterised, low strain environments, as they are much more sensitive to the exciting amplitude. This opens up the potential of harvesting usable power from smaller vibrations than previously considered viable, making these designs ideal for structural health monitoring. Small oscillations in a building's superstructure from wind loading or vehicles passing over the span of a bridge could become more suitable energy sources for remote sensor nodes. The natural development of the APEH described in this paper would be a larger scale design (with a multi-unit REHA as the auxetic region) to harvest more energy.

6. Conclusion

This paper demonstrated that use of an auxetic (negative Poisson's ratio) structure increases the power output of a strain vibration energy harvester, relative to a plain equivalent structure. Finite element modelling was used to optimise the auxetic region (a re-entrant hexagon) of the substrate. Simulation results suggested that the auxetic region concentrates strain applied to the substrate into the piezoelectric element bonded over it, and adds an additional lateral component of strain; both effects increase the power output from the piezoelectric elements.

The optimised auxetic piezoelectric energy harvesters (APEH) were manufactured, tested, and compared with equivalent strain energy harvesters with a plain substrate. When excited by sinusoidal strain of 250 με at 10 Hz, the APEHs produced up to 191 μW, compared to the plain's mere 13.3 μW. This yields a power gain of up to 14.4. The power gain factor remained approximately constant as the excitation was varied, demonstrating it is a function of the substrate geometry and is not dependant on the excitation. These characteristics of the gain were all identified by the FEM design process but the imperfect bonding between the glue (epoxy) and the constituent elements made prior prediction of power output imprecise. Modelling the imperfect bonding was achieved by using the stiffness of thin elastic layers at the glue's interfaces, and subsequently comparing the simulated and experimental outputs to obtain improved values; future models may now utilise these as their initial estimates.

7. Acknowledgements

Our sincere gratitude for the support from all our fellow members of the Energy Harvesting Group. We acknowledge financial support from the Engineering and Physical Sciences Research Council (EPSRC) of the United Kingdom, via the EPSRC Centre for Doctoral Training in Metamaterials (Grant No. EP/L015331/1). All data created during this research are openly available from the University of Exeter's institutional repository at https://doi.org/10.24378/exe.[XXXX].

8. References

[1] A. Harb, Energy harvesting: State-of-the-art, Renew. Energy. 36 (2011) 2641–2654. doi:10.1016/j.renene.2010.06.014.
[2] C. Wei, X. Jing, A comprehensive review on vibration energy harvesting: Modelling and realization, Renew. Sustain. Energy Rev. 74 (2017) 1–18. doi:10.1016/j.rser.2017.01.073.
[3] F.K. Shaikh, S. Zeadally, Energy harvesting in wireless sensor networks: A comprehensive review, Renew. Sustain. Energy Rev. 55 (2016) 1041–1054. doi:10.1016/j.rser.2015.11.010.
[4] M.Q. Le, J.-F. Capsal, M. Lallart, Y. Hebrard, A. Van Der Ham, N. Reffe, L. Geynet, P.-J. Cottinet, Review on energy harvesting for structural health monitoring in aeronautical applications, Prog. Aerosp. Sci. 79 (2015) 1–11. doi:10.1016/j.paerosci.2015.10.001.
[5] A. Somov, Z.J. Chew, T. Ruan, Q. Li, M. Zhu, Poster abstract : Piezoelectric energy harvesting powered WSN for aircraft structural health monitoring, 15th ACM/IEEE Int. Conf. Inf. Process. Sens. Networks. (2016) 1–2. doi:10.1109/IPSN.2016.7460711.
[6] EnOcean GmbH, Energy Harvesting Wireless Power for the Internet of Things, (2015) 1–7. https://www.enocean.com/en/technology/white-papers/.
[7] J. Chen, G. Zhu, J. Yang, Q. Jing, P. Bai, W. Yang, X. Qi, Y. Su, Z.L. Wang, Personalized Keystroke Dynamics for Self-Powered Human - Machine Interfacing, ACS Nano. 9 (2015) 105–116. doi:10.1021/nn506832w.
[8] ORBCOMM Inc., GT 1100 Datasheet, (2016) 2. https://www.orbcomm.com/PDF/datasheet/GT-1100-Trailer-Tracking.pdf.
[9] J. Rush, Passive Eye, Passive Eye, (2016). http://passive-eye.com/index.php (accessed May 9, 2018).
[10] T. Ikeda, Fundamentals of Piezoelectricity, 1st ed., Oxford Science Publications, 1990. doi:10.1524/zkri.1992.199.1-2.158.
[11] M. Pozzi, A. Canziani, I. Durazo-Cardenas, M. Zhu, Experimental characterisation of macro fibre composites and monolithic piezoelectric transducers for strain energy harvesting, in: Smart Struct., 2012: p. 834832. doi:10.1117/12.917094.
[12] M. Pozzi, S. Guo, M. Zhu, Harvesting energy from the dynamic deformation of an aircraft wing under gust loading, Proc. SPIE Heal. Monit. Struct. Biol. Syst. 8348 Smart Struct. 2012. (2012) pp834831–1/11. doi:10.1117/12.917039.
[13] K.E. Evans, M.A. Nkansah, I.J. Hutchinson, S.C. Rogers, Molecular network design, Nature. 353 (1991) 124–124. doi:10.1038/353124a0.
[14] S.K. Bhullar, Three decades of auxetic polymers: A review, E-Polymers. 15 (2015) 205–215. doi:10.1515/epoly-2014-0193.
[15] T.C. Lim, Analogies across auxetic models based on deformation mechanism, Phys. Status Solidi - Rapid Res. Lett. 11 (2017). doi:10.1002/pssr.201600440.
[16] M. Mir, M.N. Ali, J. Sami, U. Ansari, Review of mechanics and applications of auxetic structures, Adv. Mater. Sci. Eng. 2014 (2014) 1–18. doi:10.1155/2014/753496.
[17] K.K. Saxena, R. Das, E.P. Calius, Three Decades of Auxetics Research - Materials with Negative Poisson's Ratio: A Review, Adv. Eng. Mater. 18 (2016) 1847–1870. doi:10.1002/adem.201600053.
[18] M. Taylor, L. Francesconi, M. Gerendás, A. Shanian, C. Carson, K. Bertoldi, Low porosity metallic periodic structures with negative poisson's ratio, Adv. Mater. 26 (2014) 2365–2370. doi:10.1002/adma.201304464.
[19] L. Mizzi, K.M. Azzopardi, D. Attard, J.N. Grima, R. Gatt, Auxetic metamaterials exhibiting giant negative Poisson's ratios, Phys. Status Solidi - Rapid Res. Lett. 9 (2015) 425–430. doi:10.1002/pssr.201510178.
[20] I.G. Masters, K.E. Evans, Models for the elastic deformation of honeycombs, Compos. Struct. 35 (1996) 403–422. doi:10.1016/S0263-8223(96)00054-2.
[21] K. Alderson, A. Alderson, N. Ravirala, V. Simkins, P. Davies, Manufacture and characterisation of thin flat and curved auxetic foam sheets, Phys. Status Solidi Basic Res. 249 (2012) 1315–1321. doi:10.1002/pssb.201084215.
[22] Q. Li, Y. Kuang, M. Zhu, Auxetic piezoelectric energy harvesters for increased electric power output, AIP Adv. 015104 (2017). doi:10.1063/1.4974310.
[23] M.L. De Bellis, A. Bacigalupo, Auxetic behavior and acoustic properties of microstructured piezoelectric strain sensors., Smart Mater. Struct. (2017) 28. doi:10.1088/1361-665X/aa7772.
[24] Y. Umino, T. Tsukamoto, S. Shiomi, K. Yamada, T. Suzuki, Development of vibration energy harvester with 2D mechanical metamaterial structure, in: F. Suzuki (Ed.), Power MEMS 2017, Power MEMS, Kanazawa, 2017: pp. 1–4.
[25] J. Adeshara, Design optimization of geometrical parameters and material properties of vibrating bimorph cantilever beams with solid and

honeycomb substrates for maximum, All Theses. Pap. 1717. (2013).
[26] N. Chandrasekharan, L.L. Thompson, Increased power to weight ratio of piezoelectric energy harvesters through integration of cellular honeycomb structures, Smart Mater. Struct. 25 (2016) 045019. doi:10.1088/0964-1726/25/4/045019.
[27] T. Fey, F. Eichhorn, G. Han, K. Ebert, M. Wegener, A. Roosen, K. Kakimoto, P. Greil, Mechanical and electrical strain response of a piezoelectric auxetic PZT lattice structure, Smart Mater. Struct. 25 (2016) 015017. doi:10.1088/0964-1726/25/1/015017.
[28] Physik Instrumente, Piezo Material Data, (2011). http://www.pi-usa.us/tutorial/Piezo_Material_Datasheet_Cofefficients_Temperature_Measurements.pdf.

[1] **William J. G. Ferguson** received his MPhys in Energy Science & Technology from Heriot-Watt University in 2015, followed by taking up his current postgraduate researcher position in the Centre for Doctoral Training in Metamaterials at the University of Exeter. His main research interests are focused on improving vibration energy harvesting transducers using auxetic structures, for use in structural health monitoring.

[2] **Yang Kuang** received his B.Eng and M.Eng in Mechanical Engineering from Central South University, China, in 2007 and 2010, respectively, and his PhD in high power piezoelectric transducers from University of Dundee in 2014. He is currently working as a research fellow in the energy harvesting research group in University of Exeter. His main research interests are focused on self-power wireless sensing systems enabled by energy harvesting.

[3] **Ken E. Evans** holds the Chair of Materials Engineering and is the Dean of the College of Engineering, Mathematics and Physical Sciences. He is also the Director of Exeter Advanced Technologies and Director of the Centre for Additive Layer Manufacturing. His research is on the theoretical and experimental investigation of novel materials, including their processing, fabrication, structure and properties and in their engineering and industrial applications. He is an acknowledged international expert on auxetic materials. Areas of interest include blast mitigation fabrics, synthetic skin, 'smart' materials, structural honeycombs and foams, and open framework ceramics.

[4] **Christopher W. Smith** is Associate Professor in Functional Materials and Deputy Associate Dean for Research (Industry). He graduated from the University of Leeds in 1992 and remained there to do a PhD in Biomaterials, graduating in 1995. He then worked as a post-doctoral research fellow at the Universities of York and Exeter. He was appointed Lecturer in Mechanical Engineering in January 2000, Senior Lecturer in 2006, and Associate Professor in Functional Materials in 2008. His research interests are in adding functionality into structures and materials, most recently focused on passive lightweight vibration damping technology, and wear of friction contacts.

[5] **Meiling Zhu** received her BEng degree in 1989, MEng in 1992, and PhD in 1995 at Southeast University, Nanjing, China. She currently holds the Professor and the Chair in Mechanical Engineering and the Head of Energy Harvesting Research Group in the University of Exeter in the UK. Prior to joining the University of Exeter, she worked in a number of Universities including Cranfield University), the University of Leeds; Stuttgart Universität; the Hong Kong University of Science and Technology. Her current research interests are in the area of piezoelectric energy harvesting powered wireless sensor nodes for applications.

Declarations of interest: none

Supplementary Material

A. Parametric Study of the Auxetic Region

The key parameters defining the shape of auxetic region are the beam width, t_b, cell angle, α, the crossbeam length, *cb*, and the filleting radius in all the corners, *r*. A parametric study in COMSOL Multiphysics® 5.3 was used to identify the optimum values, as judged by their ability to produce the highest power output without excessive stress. Multiple such studies were carried out with various starting points and differing routes through the four given parameters to attempt to find a global optimum; we here present one such route. For all the simulations, the excitation strain was 250 με at 10 Hz. When each of the four parameters was varied, the others were kept constant at either the initial values or the previously optimised values once available.

For all the simulations performed below, the peak stress in the piezoelectric element was found to be less than a third of its tensile strength (35 MPa), while the peak stress in the substrate can excess its yield strength (280 MPa). Therefore, the peak stress of substrate is presented while the peak stress in the piezoelectric element is omitted.

A1. Beam Width

The effects of the beam width, t_b, on the power output and the peak stress of the substrate are shown in Figure A1(a). The average axial and lateral stresses in the piezo are shown in Figure A1(b). α and *r* were kept constant at 35° and 0.3 mm, respectively. No crossbeam was used. As the beam width increases, the power first increases and then decreases after reaching the maximum of 51 μW when t_b is 2.4 mm. The increase of the power with t_b is due to the greater rigidity and contact area granting additional authority for the beams to strain the PZT. Beyond 2.4 mm however, the beams lose flexibility, thus reducing the stress concentration into the auxetic region and the strain passed into the piezo. Figure A1(b) shows how the beam width affects both the axial and lateral components of the piezo stress in a similar way, indicating beam width primarily affects the overall stiffness of the auxetic region.

The peak stress of the substrate generally increases with t_b, even while the input strain is constant. This can be attributed to the additional material in the corners of the auxetic region, making flexing more difficult. To help keep the substrate within the yield stress limit we elected to use t_b = 2 mm. The use of thinner beams is less ideal when considering only the power output, but will allow more space for a crossbeam; as discussed in A3 below.

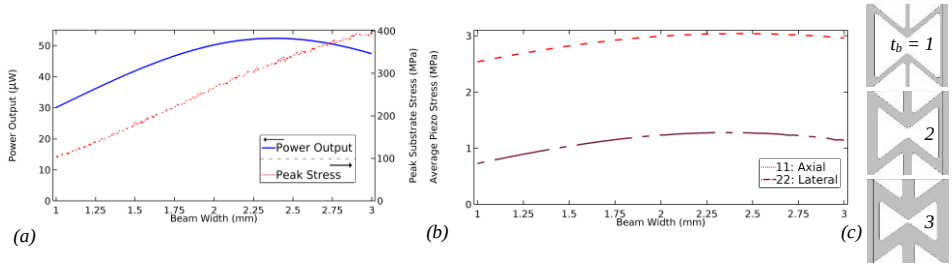

Figure A1: (a) Simulated power output from PZT (solid) and peak stress in substrate (dotted) against beam width, t_b; (b) Average piezo stresses in axial (dashed) and lateral (dot-dashed) directions against t_b. (c) Selected examples of t_b's effect on the auxetic region's structure.

A2. Re-Entrant Cell angle

How deeply the unit re-enters itself may be defined by either the cell angle, α, or the equivalent deformation length, d, both shown in Figure 3(b). It is related to how far the unit could potentially expand outwards when the structure is placed under tension. In general, the more the auxetic region is able to expand under tension, the more lateral strain (and thereby additional power) in the piezoelectric element). As the corners become more acute, stress is concentrated into these corners, but as the cell angle increases so too does the length of the beams; this can help distribute the stress across a wider area. This two factors explain the initial rise and subsequent fall in the peak stress seen in Figure A2(a) as the angle is increased.

The optimum for power output occurs at 30˚ (6.3 mm). Figure A2(b) shows that most of the power gain associated with the deformation comes from the lateral stress component, with only a small increase found due the increased axial stress (due to the reduced stiffness of the auxetic region with sharper angles). Our selected deformation is 33˚ (7.4 mm) as, despite the small loss in power, the lower peak stress is desirable.

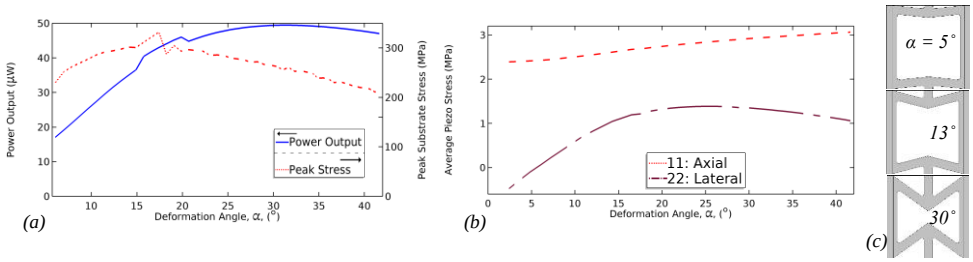

Figure A2: (a) Simulated power output from PZT and peak stress in substrate against cell angle, α; (b) Average stresses in PZT in axial and lateral directions against α; (c) Examples of α's effect on the structure.

A3. Crossbeam Length

A crossbeam is added to the free ends of the REHA to provide additional grip to the piezo-elements and thus aid the lateral strain transfer. Figure A3(b) demonstrates that all the benefit from this comes through the lateral stress component. The substrate's peak stress remains relatively stable throughout. From Figure A3, the most power may be obtained when the crossbeam is as wide as will physically fit into the available space (12 mm long). Using this full width would be impossible to manufacture by laser cutter, as the space between the crossbeam tip and the angled beams of the auxetic region would be too narrow. The chosen length is therefore 11 mm, around 91% of the available space.

Commented [DMOU1]: Optional:
If the crossbeam is too long, the stress in the piezo in these areas would be increased to an existent that, while still around a third of the PZT's strength, would become the areas most susceptible to cracking (rather than the centre).

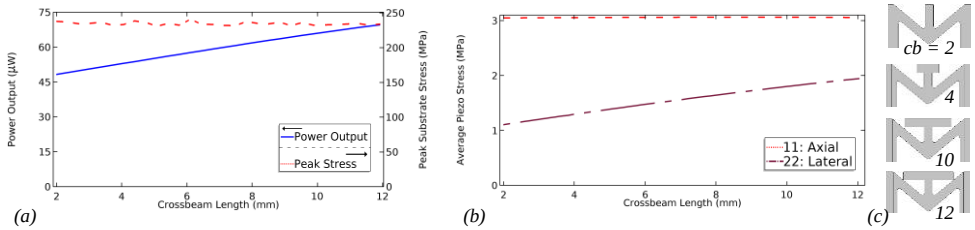

Figure A3: (a) Simulated power output and peak stress in substrate against crossbeam length, cb; (b) Average stresses in PZT in axial and lateral directions against cb; (c) Examples of cb's effect on the structure.

A4. Filleting Radius

Any sharp corners in the auxetic region, especially those flexing outwards, are prone to excessive concentration of stress. In Figure A4, we show the simulated effect of filleting these corners to different radii, from the minimum attainable by most laser cutters (0.1 mm) up to the maximum curvature that fits behind the crossbeams (1.33 mm). The peak substrate stress is highest when the radius is smaller, as this focuses all the force from the beams' flexing into a smaller area. When the radius is sufficiently large that the extra material in the corners impedes the flexing of the region the peak stress increases slightly. This can is shown in Figure A4(a) above 0.6 mm.

Figure A4(b) shows that the filleting radius affects both axes of the piezo relatively equally. The gradual decrease with larger radii indicates *r*'s effect on power is primarily driven by the overall stiffness of the auxetic region; due to the added material in the corners. To maintain as much power as possible, while minimising the substrate's stress, we've selected a filleting radius of 0.5 mm. This concludes this derivation of the dimensions listed in Table 1.

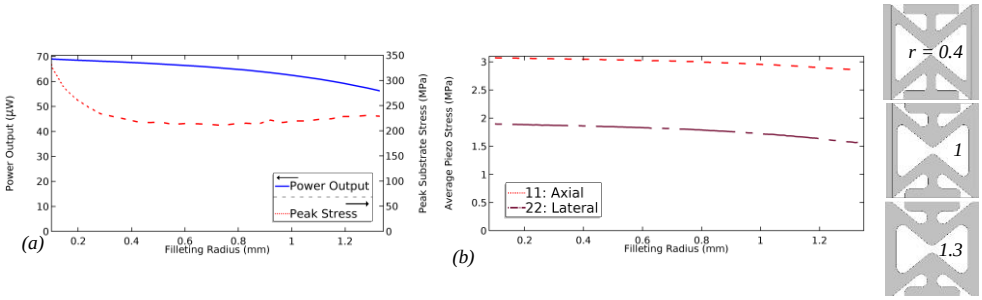

Figure A4: (a) Simulated power output and peak stress in substrate against filleting radius, r; (b) Average stresses in PZT in axial and lateral directions against r; (c) Examples of r's effect on the structure.